Some Problems in the Oxidative Addition and Binding of an Ethylene to a Transition-Metal Center

Jérôme Silvestre,[1a,b] Maria José Calhorda,[1a,c] Roald Hoffmann,*[1a] Page O. Stoutland,[1d] and Robert G. Bergman[1d]

Department of Chemistry and Material Sciences Center, Cornell University, Ithaca, New York 14853, Department of Chemistry, University of California, Berkeley, California 94720, and Materials and Molecular Research Division, Lawrence Berkeley Laboratory, Berkeley, California 94720

Received January 9, 1986

Molecular orbital calculations have been carried out on the potential energy surface of the system $CpIrL(C_2H_4)$ (L = phosphine). The geometrical and electronic characteristics of the η^2-olefin and vinyl hydride complexes are examined in some detail. The olefin complex is found to have a slightly lower energy than the vinyl hydride, in agreement with experiment. Different routes are studied which lead to the oxidative addition product from the 16-electron fragment and an ethylene. It is found that an M···H–C linear approach is favored, coupled with a very specific orientation of the ethylenic π system. This results from both electronic and steric requirements. A relatively small barrier is computed for the process, and the experimentally observed competition between vinyl hydride formation and direct ethylene addition is discussed. Calculations have been performed to ascertain the existence of a separate transition state taking the η^2-bound olefin into the vinyl hydride. The computations suggest the existence of two distinct transition states. The influence of substituents and particularly steric effects is analyzed. It is shown how an increase in the size of the ligand affects the shape of the surface and more specifically narrows the energy channels governing conformational changes as well as product formation.

The making and breaking of C–H bonds mediated by transition-metal fragments has emerged in the last decade as a major goal of experimental organometallic chemistry.

Due to an increased interest in the activation of alkanes,[2] an enormous amount of data has been generated, dealing with intra- and/or intermolecular C–H oxidative addition[3] as well as with the so-called "agostic" interactions.[4] Theoreticians have also tried to contribute their share toward an understanding of the phenomena.[5]

A related process is that of the activation of arene (or more generally olefin) C–H bonds. It might seem that the reaction would occur more easily since a reasonable starting point[6] is a precoordinated olefin at an electron-deficient transition-metal center. This assumption was made in a number of different studies[7] and justified[8] experimentally by Jones and Feher for the $CpRhPR_3$/benzene system. Perhaps we should mention here a related series of reactions, those featuring an oxidative addition of α-unsaturated C–H bonds. They involve [1,*n*]-sigmatropic shifts occurring on π-bonded polyenes. In these systems, the migrating hydrogen is believed to accomplish the transit via the metal center, reinserting in a subsequent step.[9]

Scheme I

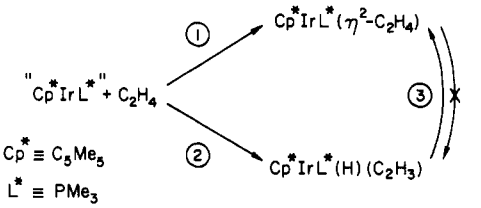

Interestingly, the requirement of π precoordination of the olefin was called into question recently[10] by Bergman and co-workers. The essence of their results can be cast into Scheme I as shown. The 16-electron Cp*IrL* fragment is generated by reductive elimination of cyclohexane out of $Cp^*IrL^*(H)(C_6H_{11})$ at ~140 °C. The η^2-bound olefin and the vinyl hydride complexes are formed in a 34/66 radio, which represents a kinetic product ratio. At temperatures higher than those required for the reductive elimination, the vinyl hydride is converted quantitatively to the η^2-olefin complex. Control experiments rule out elimination of C_2H_4 from the vinyl hydride and recombination. These facts taken at face value indicate (i) that the η^2-olefin system is thermodynamically more stable than the vinyl hydride complex, (ii) that there is actual competition between the η^2-olefin complex formation and C–H oxidative addition leading to the vinyl hydride, (iii) that we may have at hand at least three different transition states corresponding to steps ①, ②, and ③ in Scheme I, and (iv) that the π complex does not have to lie on the reaction path leading to olefinic C–H oxidative addition.

In this contribution we would like to shed some light on the above points (i) to (iv). Our conclusions are based on symmetry and overlap arguments supplemented by computations at the extended Hückel level.[11] The paper is

(1) (a) Cornell University. (b) Present address: Institut de Recherche sur la Catalyse, CNRS, Labo. de Chimie Theorique: 2, Av. A. Einstein, 69626 Villeurbanne, France. (c) Permanent address: Centro de Quimica Estrutural, Instituto Superior Tecnico, 1096 Lisboa Codex, Portugal. (d) University of California.

(2) See: Muetterties, E. L. *Chem. Soc. Rev.* **1982**, *11*, 283 for the relevant references.

(3) (a) Crabtree, R. H.; Holt, E. M.; Lavin, M.; Morehouse, S. M. *Inorg. Chem.* **1985**, *24*, 1986 and references therein. (b) See also ref 5a.

(4) Brookhart, M.; Green, M. L. H. *J. Organomet. Chem.* **1983**, *250*, 395.

(5) (a) Saillard, J.-Y.; Hoffmann, R. *J. Am. Chem. Soc.* **1984**, *106*, 2006. (b) Shustorovich, E. *J. Phys. Chem.* **1983**, *87*, 14. (c) For a treatment of agostic interactions with references to other papers see: Eisenstein, O.; Jean, Y. *J. Am. Chem. Soc.* **1985**, *107*, 1177.

(6) Chatt, J.; Davidson, J. M. *J. Chem. Soc.* **1965**, 843. Parshall, G. W. *Homogeneous Catalysis*; Wiley: New York, 1980; p 123. Parshall, G. W. *Catalysis* **1977**, *1*, 334.

(7) Muetterties, E. L.; Bleeke, J. R. *Acc. Chem. Res.* **1979**, *12*, 329. Jones, W. D.; Feher, F. J. *J. Am. Chem. Soc.* **1982**, *104*, 4240. Fryzuk, M. D.; Jones, T.; Einstein, F. W. D. *Organometallics* **1984**, *3*, 185. For an example on a dirhenium system, see: Nubel, P. O.; Brown, T. L. *J. Am. Chem. Soc.* **1984**, *106*, 644.

(8) Jones, W. D.; Feher, F. J. *J. Am. Chem. Soc.* **1985**, *107*, 1650.

(9) Selected contributions include: Green, M.; Hughes, R. P. *J. Chem. Soc., Dalton Trans.* **1976**, 1907. Johnson, B. F. G.; Lewis, J.; Ryder, J. E.; Twigg, M. V. *Ibid.* **1976**, 421. Whitesides, T. H.; Arhart, R. W. *Tetrahedron* **1972**, 297. Krusic, P. J.; Briere, R.; Rey, P. *Organometallics* **1985**, *4*, 80. Murr, N. E.; Payne, J. D. *J. Chem. Soc., Chem. Commun.* **1985**, 162. Werner, R.; Werner, H. *Chem. Ber.* **1984**, *117*, 161.

(10) Stoutland, P. O.; Bergman, R. G. *J. Am. Chem. Soc.* **1985**, *107*, 4581.

0276-7333/86/2305-1841$01.50/0 © 1986 American Chemical Society

organized as follows. First we shall deal with the geometry and electronic structure of the three "end points" of the surface, namely, the 16-electron fragment, the η^2-bound C_2H_4, and the vinyl hydride complex. Next we look at the formation of two complexes and delineate several routes for both ② and ③—see Scheme I. Finally substituent effects are discussed from both electronic and steric points of view. All the technical details relevant to the calculations may be found in the Appendix.

A word of caution is required at the beginning. The reactions that we wish to study involve the breaking and making of bonds. The extended Hückel method is not very good at the energetics of such processes. Our results are not likely to be very reliable; nevertheless, we think that they lead to interesting considerations, questions of chemical significance.

Geometry and Electronic Structure of Three Points on the Surface

Central to this work is the CpIrL fragment **1**. A detailed exposition of its valence molecular orbitals may be found elsewhere.[12] Our initial calculations use C_5H_5 for the Cp

1

ring and PH_3 for the phosphine. Later the full steric bulk will be restored by incorporation of methyl groups, on Cp and the phosphine.

Let us first look at the electronic structure of the η^2-olefin, **2**, and the vinyl hydride, **3**, complexes. At this point

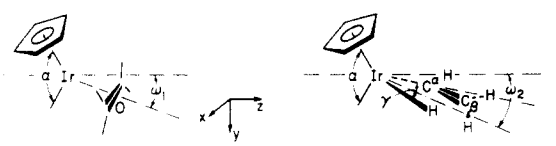

2 **3**

α and $\omega_{1,2}$ (defined in **1**–**3**) are fixed at 135° and 0°, respectively. In **3**, γ is set at 80°. The angle α is that between the Ir–centroid and Ir–P bonds and defined in such a way that its bisector lies parallel to the z axis. ω_1, also in the yz plane, measures the deviation of the Ir–(center of ethylene) vector away from $\bar{z}$. Simultaneously ω_2 measures the deviation of the C_α–Ir–H bisector away from $\bar{z}$. The orientation of the C_α–C_β bond with respect to the Cp and the hydride is for the moment that indicated in **3**. We will soon give the molecule additional degrees of freedom.

In Figure 1 we show side by side the MO pattern of **2** and **3** in the geometry described above. For **2**, the four olefinic C–H bonds are still in the xy plane, not puckered. In the middle of Figure 1 sit the orbitals of **1** (α = 135°). In this d^8-ML_4 unit all orbitals but 3a′ are occupied.[13] They interface at right with π and π^* of C_2H_4. On the extreme left-hand side of the figure we have indicated π and π^* of the vinyl fragment and the two σ donors, one being centered on the hydrogen, ψ_1, and symmetric with respect to the pseudo yz plane of symmetry and the other localized on an sp^2 hybrid of the α vinylic carbon and "antisymmetric" with respect to yz, ψ_2. Obviously in this case the Ir atom is in a d^6 configuration, as indicated in Figure 1, and within this formalism 2a″ is empty.

The right-hand side of Figure 1 is self-explanatory. The Dewar–Chatt–Duncanson model operates fully: π donates into 3a′ (which gets populated with 0.468 electron) and 2a″ back-donates into π^*, receiving 0.515 electron. Secondary mixing due to the low symmetry (C_s) moves around the three low-lying d orbitals a little.

The left-hand side of Figure 1 is slightly more complicated, due to the absence of symmetry. Still, ψ_1 is pushed down by a mixture of 1a′ and 3a′, whereas ψ_2 interacts with 1a″; both orbitals are filled, and it is only secondary mixing of 2a″ which maintains the resulting antibonding MO at a reasonably low energy. The vinyl π and π^* orbitals interact a little with the metal, primarily via 2a′. The reason for this may be traced to the isolobal relationship between the d^6 CpIrL and CH_2^{2+} or CH^+. The vinyl hydride complex is isolobal with the allyl anion, as shown in **4**. One should find in **3** a molecular orbital analogous to

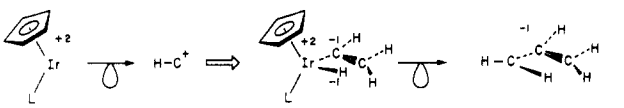

4

the π-nonbonding MO of a $C_3H_5^-$ unit, occupied due to the negative charge. This orbital exists and lies next to the HOMO in Figure 1; its shape is depicted in **5a**, whereas

5

5b shows the HOMO of $C_3H_5^-$. Molecular orbital **5a** is exclusively localized on the metal and the β-carbon, 80% and ~20%, respectively. Its topology results from in-phase mixing of π^* and out-of-phase mixing of π, in turn cancelling out the density on C_α.

Let us now turn to the energetics of **2** and **3**. For this purpose some geometry optimization was carried out on both systems. First of all, one may optimize the σ interactions involving 3a′. 3a′ obviously dictates a privileged direction or a direction of maximum σ overlap. Figure 2 shows a plot of 3a′ in the yz plane and indicates at a glance why ω_1 and ω_2 must optimize at a value different from 0°. The direction of maximum electron density of 3a′ lies ~18° away from the bisector.

For a fixed Ir–(midpoint of the C–C double bond) distance (2.0 Å) one may vary three geometrical parameters: the orientation of the double bond, ω_2 (see **2**), and the puckering of the hydrogens. A previous study by one of us[14] shows that the orientation of an ethylene bound to a ML_4 unit is determined primarily by electronic factors. In the case under consideration both electronic and steric factors will favor the orientation shown in **2**. The alternative upright conformation (C–C in yz plane) would engender steric problems between one carbon and the Cp ring. Also, better back-bonding is achieved via 2a″ rather than 2a′. Independent optimization of ω_1 and the puckering angle of the ethylene hydrogens puts the energy of

(11) Hoffmann, R. *J. Chem. Phys.* **1963**, *39*, 1397. Hoffmann, R.; Lipscomb, W. N. *Ibid.* **1962**, *36*, 3179, 3289; **1962**, *37*, 7872.

(12) (a) Hofmann, P. *Angew Chem.* **1979**, 591. Pinhas, A. R.; Albright, T. A.; Hofmann, P.; Hoffmann, R. *Helv. Chim. Acta* **1980**, *63*, 29. (b) Hofmann, P., Padmanabhan, M. *Organometallics* **1983**, *2*, 1273.

(13) For the time being, a singlet configuration is assumed for **1**, since we are interested at this point in the "static" electronic structure of **2** and **3**. The electron partitioning is conceptual at this stage.

(14) Albright, T. A.; Hoffmann, R.; Thibeault, J. C.; Thorn, D. L. *J. Am. Chem. Soc.* **1979**, *101*, 3801.

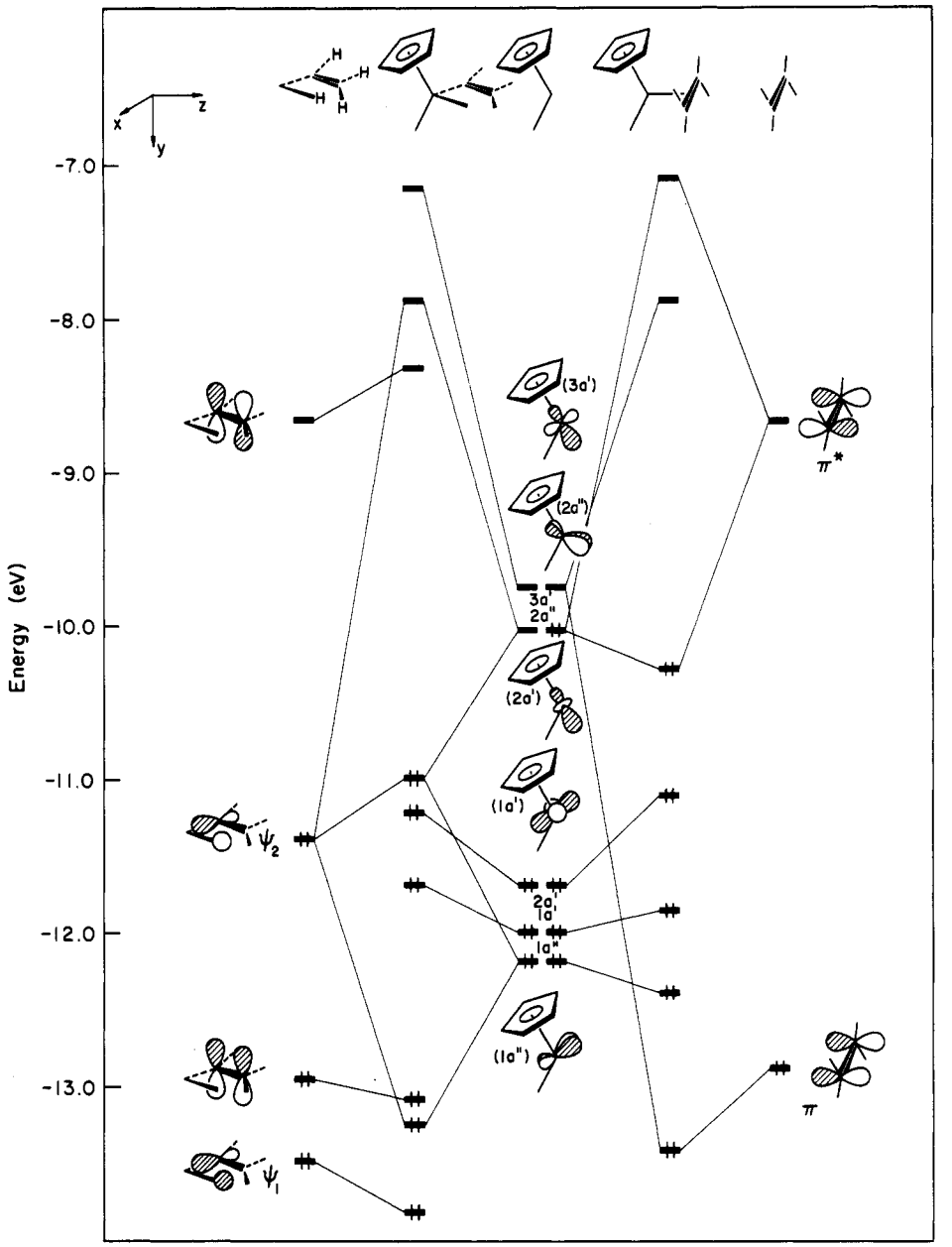

Figure 1. Construction of the MO diagram for **2** (right) and **3** (left).

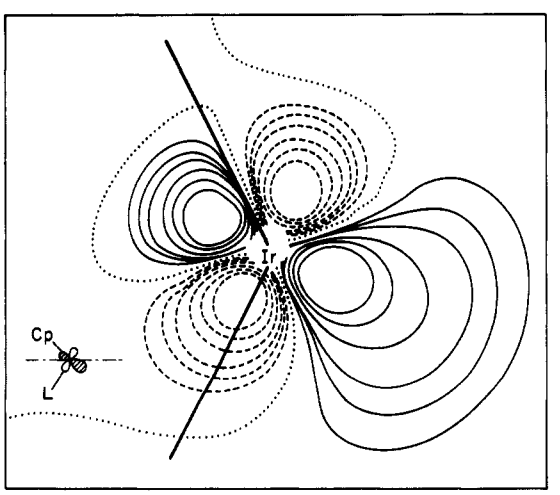

Figure 2. A contour plot of molecular orbital 3a′ of the CpIrL fragment. Solid and dashed lines represent positive and negative values, respectively. The dotted lines are the nodal surfaces.

2 ~35 kcal/mol below that of **2** with $\omega_1 = 0°$ and a planar C_2H_4.

From now on it will be useful to have a common energy scale for all the points on the potential surface of the $CpIrL/C_2H_4$ system. The zero of energy is taken as the sum of the energies of CpIrL and C_2H_4 set at an infinite distance from each other. On this energy scale, the optimized ethylene complex lies at −40 kcal/mol.

A complete geometry optimization of the vinyl hydride is computationally out of reach, at least for us. Some assumption had to be made and the Cp–Ir–P angle was kept at 135°. The H–Ir–C_α angle was set at 80°, and bond distances were not varied. The optimization consisted of an independent variation of ω_2 and θ defined in **6a** and **6b**.

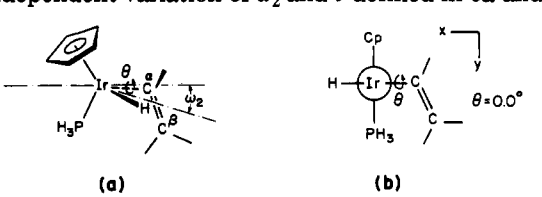

6

In the latter view the molecule is projected onto the xy plane; this illustrates further the geometrical meaning of

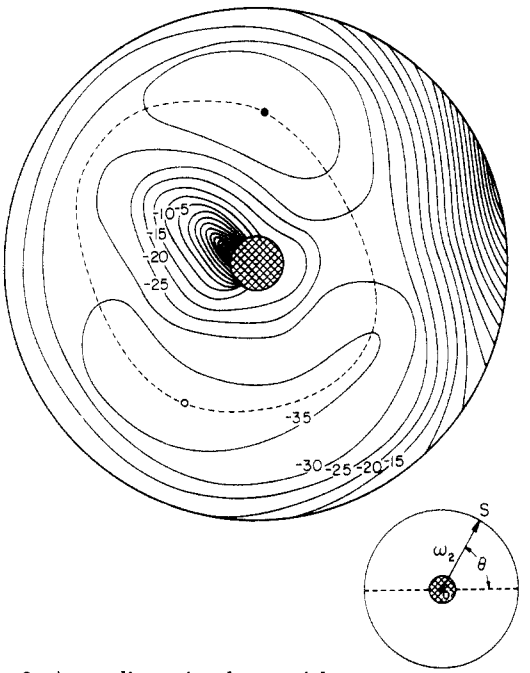

Figure 3. A two-dimensional potential energy surface optimizing independently θ and ω_2 defined in **6** (see text) for $(C_5H_5)Ir(PH_3)(H)(C_2H_3)$. Contours are in kilocalories per mole.

the angle θ. The angle ω_2 was introduced earlier in the text; see **3**. The angle θ measures the dihedral angle made by the C_α–C_β bond with respect to the y axis sticking out of the iridium center. Figure 3 presents the results of the calculations for the two-dimensional surface with ω_2 and θ as variables. The range over which θ was varied (0–360°) suggested to us the idea of plotting the contours in polar coordinates defined at the bottom right of Figure 3. The angle ω_2 was allowed to go from 0 to 30° with a 7.5° increment. Only positive ω_2 was considered; this will be justified by the results we show. ω_2 is represented by the length of the vector $\overline{OS}$ (Figure 3). The angle θ monitors the direction of that $\overline{OS}$ vector. The central cross-hatched circle serves via its external boundary to vary θ for ω_2 equal to 0°. The contours are separated by 5.0 kcal/mol and refer to the zero of energy (vide supra). The dark circle corresponds to the global minimum and the open circle to the local minimum. The dashed line follows the least-energy paths for interconversion of the two minima.

The surface presents several interesting features. First one may see clearly the influence of the Cp and PH_3 groups upon rotation around the Ir–C_α bond, i.e., variation of θ. At large ω_2—the vinyl fragment is down—a high-energy region is encountered in the neighborhood of $\theta = 0°$; this is the wicked influence of the phosphine. Conversely, when ω_2 is small (the Ir–C_α bond is moved up), a high-energy region is encountered for $\theta = \sim 180°$ because the Ir–C_α bond is not in the yz plane.

The two minima are almost equi-energetic (at ~39 kcal/mol), and two channels exist to go from one to the other. Amazingly enough the potential is softer on the Cp side than on the phosphine side. Note also that it does not cost much energy for the C_2H_3 unit to oscillate around the best values of θ; the potential about both minima is rather flat. We shall see how restoring the full steric bulk of the real ligands (C_5Me_5, PMe_3) alters dramatically this surface. Perhaps should we take note here of the fact that the X-ray structure[10] of the vinyl hydride complex is found to lie closely within the region of our local minimum.

Finally it is important to note that our calculations, within the geometrical constraints chosen, put the olefin complex at a small 1.0 kcal/mol lower in energy than the vinyl hydride. Given the approximations used in this work the fact that we obtain the "right" energy ordering, since the η^2-olefin was found to be the thermodynamic product,[10] is probably fortuitous. However, the computations do show that the two systems are closely spaced on the energy scale.

Formation of the Vinyl Hydride and η^2-Olefin Complexes

Let us first consider the formation of the vinyl hydride. There are obviously a number of different geometrical ways in which the oxidative addition could be accomplished. Two types of approach of C_2H_4 toward the metallic center may be envisioned: The C–H bond might be perpendicular to the metal midpoint of C–H axis, **7**, or both are colinear, **8**.

7 **8**

In certain regions of the potential energy surface **7** will be less favorable than **8**, and in others **7** needs to be examined in detail. Four possibilities for **7** must be considered, and these are depicted in **9a–d**, looking down the

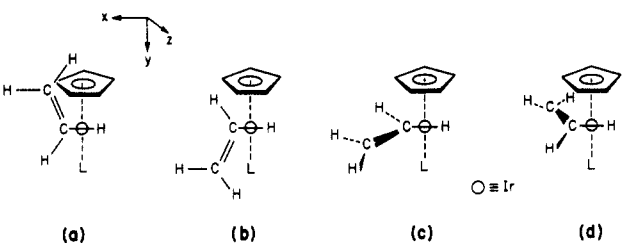

9

C–H midpoint–Ir bond. **9a,b** presents the C_2H_4 unit in the xy plane, whereas in **9c,d** the ethylene comes in the xz plane. It does not take many exploratory calculations to realize that **9a** and **9d** are quite unfavorable, because of steric hindrance. Both **9b** and **9c** would be viable possibilities, but taking C_2H_4 from infinity all the way to the oxidative addition product involves an energy barrier of ~55 kcal/mol. Incidentally, the perpendicular approach (**9b**) turns out to be slightly favored over the parallel one (**9c**) due to a faster growing overlap population between the metal and the incipient α-carbon. This in turn can be traced back to a better interaction between the iridium and the ethylene π system. This difference between the two orientations will become important in the forthcoming discussion.

The relatively high barrier computed for all routes of type **7** naturally led us to consider linear approaches **8** as further possibilities. This mode of attack had also come to the fore in studies of C–H activation of methane.[5a]

Again several geometrical alternatives need to be examined. We looked in some detail at three of them, the most plausible chemically, and these are schematically indicated in **10a–c**. In **10a**, the incoming ethylene lies in the yz plane, whereas it lies perpendicular to it (i.e., parallel to xz) in **10b,c**. Returning to **6**, the vinyl hydride geometries in **10a**, **10b**, and **10c** correspond to $\theta = 0°$, 270° and 90°, respectively. Two geometrical parameters are important in what follows and are defined in **11**. The distance d corresponds to the Ir···H length, whereas ω_3 measures the angle made between the M···H–C axis and the CpIrL bissector.

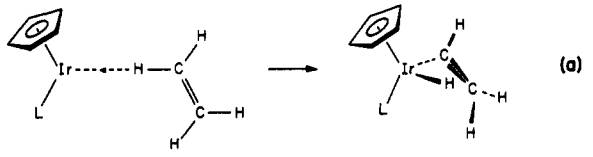

10

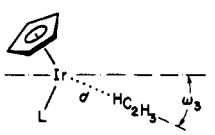

11

Let us first position ourselves at $\omega_3 = 0°$ and bring up C_2H_4 as in, say, **10a**. A relatively flat potential exists for this motion, depicted in **12**. Keeping an undistorted

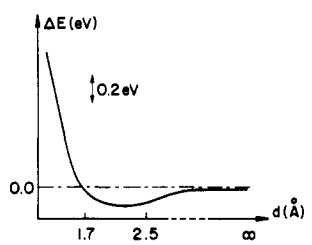

12

ethylene, it is not until one shrinks *d* to less than 1.7 Å that some severe repulsion appears. A very shallow minimum shows up at ~2.5 Å. A similar curve is obtained for **10b** and **10c**. Basically, the oxidative addition *per se* could start anywhere between 2.5 and 1.7 Å.

Next we computed a series of two-step, one-dimensional surfaces in which first an undistorted C_2H_4 is brought up to 2.0 Å of the iridium atom and then the vinyl hydride is generated in a concerted way by means of a concomitant swinging of C_2H_4 and stretching of the C–H bond. The whole process is illustrated in a series of snapshots in Figure 4 for **10a**. The calculations were performed at $\omega_3 = 0°$ and 18° and are gathered in Table I. One can see that despite the fact that the orientation resulting from **10a** is not the most stable (see Figure 3), the corresponding path is the least energetic one. We return to this point shortly.

For now we would like to point out that the topology we used to mimic the path of the reaction follows closely that reported[3a] by Crabtree and co-workers. They have nicely mapped out from a compilation of X-ray structures a likely trajectory for oxidative addition of a C–H bond on a mononuclear transition-metal fragment. However, we hasten to mention that the computed barrier can be

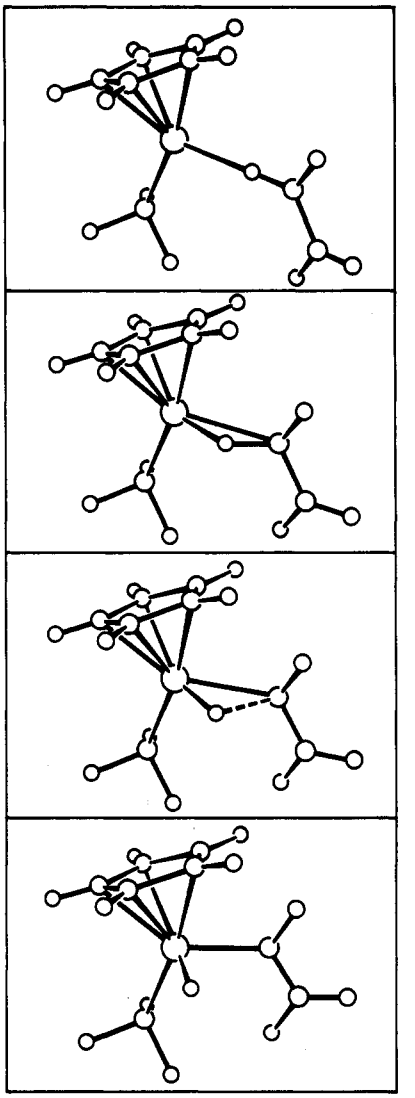

Figure 4. Snapshots of the computed reaction path **10a**.

Table I. Activation Energies for Vinyl Hydride Formation[a]

geometry ω_3	10a	10b	10c
0°	23	40	28
18°	17	30	31

[a] The zero is still the sum of the CpIrL and C_2H_4 energies; numbers are in kcal/mol.

lowered by another 7 kcal/mol if the C–H bond is brought down to 1.7 Å before starting to be rocked and cleaved. The reason for this additional gain in energy lies in the potential energy curve shown in **12**. At 1.7 Å substantial Ir–H bonding is turned on, and this favorable interaction makes up for part of the destabilization associated with the eventual C–H bond rupture. Schematically, one can summarize this argument by superimposing the potential for C–H dissociation onto that generated by a decrease of *d*, that is **12**. This is shown diagrammatically in **13**; the barrier for dissociation is lowered by "prebonding" between the metal and the hydrogen.

Can we trust this lower barrier, down to near 10 kcal/mol for C–H insertion? We are not at all certain that we can. The extended Hückel method is just not very reliable, and it seems to us that the M···H distance of 1.7 Å in the neighborhood of the minimum of **12**, close as it is to a normal metal–hydride equilibrium distance, is just too short. On the other hand, not only is the computational method not reliable, but also not all degrees of freedom

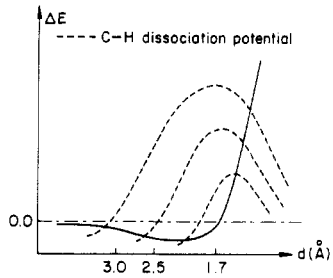

13

were varied. It could be that the barrier for insertion is less than 10 kcal. Unfortunately we have to remain uncertain on what will turn out to be a crucial magnitude.

The bonding characteristics of the reaction path are detailed in Figure 5. The path is that of **10a** with $\omega_3 = 0°$ and $d = 1.7$ Å. The vertical dashed line separates the "approach" step from the next one, the insertion. The slight discontinuities in the curves at this point result from our choice of two independent steps. The same discontinuity appears in the appended plot of the positions of the metal, α-carbon, and hydrogen in the plane defined by these three atoms. A smoother trajectory such as the one rigorously analogous to that described by Crabtree[3a] would smoothen the curves. Note the fairly large positive overlap population between the iridium and the hydrogen at 1.7 Å; remember that at this point the C–H bond is still intact. Conversely the C–H bond weakens already at this distance, as discussed in the preceding lines.

Backtracking a little to Table I, we believe that the preference of the insertion in the "perpendicular" mode **10a** is favored over that in **10b** and **10c** because of initially better bonding between the α-carbon and the metal. This is attained by interaction between the π^* orbital of C_2H_4 and 2a″ in the early stages of the process. The combination at work is a mixture of 3a′, 2a″, and π^* to produce **14**, shown in a top view. Some back-bonding is turned on in **14**. In support for this argument we offer the observations

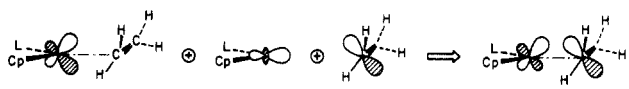

14

of (i) a faster buildup of positive charge at the metal in **10a** and then **10b** and **10c** and (ii) a more important weakening of the π bond in **10a** than in the other two geometries.

It appears from these considerations and numerical results that the oxidative addition to produce the vinyl hydride is electronically favored to occur via **10a**, the perpendicular approach. Also a barrier as small as 10 kcal/mol is computed (with limited geometry optimization) to generate the upright vinyl complex, which can collapse to the ground state via the channel described in Figure 3. We shall see in a later section how steric factors will perturb this general picture.

Let us now turn to the formation of the olefin complex. We start here with the computational results which tell us flatly that condensing the 16-electron CpIrL fragment and C_2H_4 is a process that does not involve any activation energy. This finding is not unexpected; it is only somewhat disturbing in relationship to the computed barrier to the competing oxidative addition reaction discussed above, given the 66/34 mixture of the vinyl hydride/η^2-olefin found experimentally.[10] In terms of an orbital analysis one

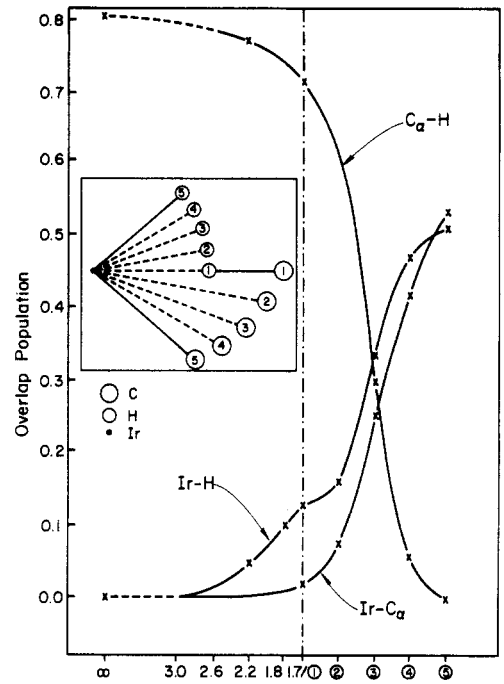

Figure 5. Selected overlap populations for the oxidative addition **10a**. The atomic motions during the second step, 1 → 5, are indicated in a box.

realizes that there should not be much of a barrier to combination of the two units since the CpIrL fragment presents a nice empty hybrid, 3a′, just ready to accept the flow of electron density from the ethylene π orbital. Thus, taking the calculational results at face value leads to a contradiction with experiment.

However, we may step back and notice that two factors, not dealt with in the one-electron model used in this work, can contribute to making the oxidative addition and the olefin complex formation competitive. These are the influence of the spin state of the species involved and the effect of the entropy contribution to the free energy of activation. The former point is discussed next, whereas the latter is taken up later when steric factors are analyzed.

Whenever one deals with a d^8-ML_4 fragment in C_{2v} symmetry, **15a**, the question comes up of its spin state.[12]

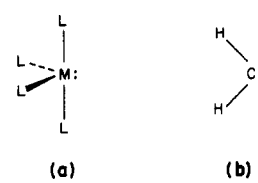

15

This in turn arises because of the proximity of 2a″ and 3a′ (b_2 and a_1 in C_{2v}) in the molecular orbital pattern of this type of fragment;[15] see Figure 1. The same kind of uncertainty exists for the isolobal[16] methylene **15b** and leads us to look back at the behavior of CH_2 in organic chemistry. The methylene fragment CH_2 is known to add across C–H bonds of hydrocarbons.[17] The reaction may be a direct insertion in the case of a singlet methylene or follow an abstraction–recombination type of mechanism when CH_2 is in the triplet state. In addition, a methylene unit has a well established propensity to add to olefinic double bonds.

(15) Albright, T. A. *Tetrahedron* **1982**, *38*, 1339.
(16) Hoffmann, R. *Angew Chem., Int. Ed. Engl.* **1982**, *12*, 711.
(17) See, for instance: Wentrup, C. *Reactive Molecules*; Wiley: New York, 1984.

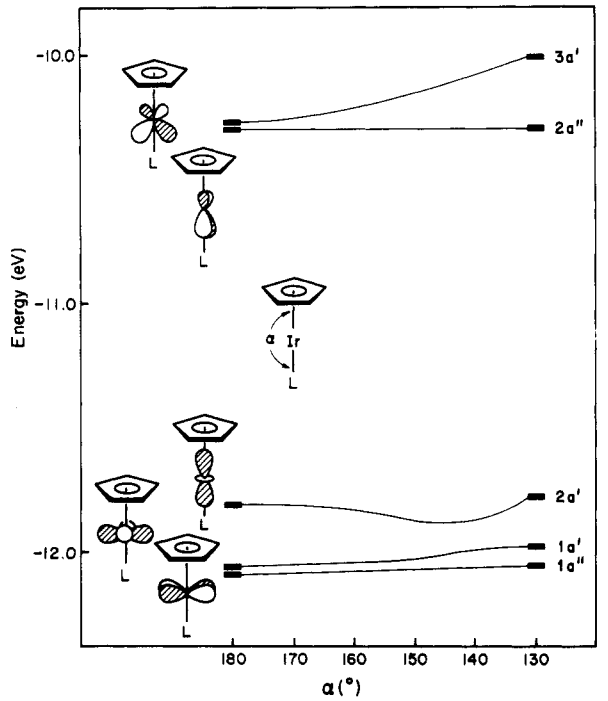

Figure 6. Walsh diagram for bending the CpIrL fragment.

The CpIrL fragment behaves just the same way. Figure 6 shows a Walsh diagram for changing α, the Cp midpoint–Ir–PH_3 angle defined in **1**. Note the near degeneracy of 3a′ and 2a″ over a large range of α. We would expect the ground state of CpIrL to be a triplet at $\alpha = 130°$. Initial SCF calculations by Veillard and Dedieu indicated a singlet ground state,[18,19] but the triplet is close by in energy and could conceivably be the ground state.

But the CpIrL fragment is likely to be *generated* in the singlet state since it is produced in solution by reductive elimination of cyclohexane out of $CpIr(H)(C_5H_{11})$. We believe that from that point on two things may happen that split the overall CpIrL population: direct addition of the singlet to the π system of C_2H_4 and formation of the η^2-bound olefin complex, competing with rapid intersystem crossing producing a triplet state complex which inserts across one olefinic C–H bond via a diradical type of mechanism. The radical components may, however, be hard to detect experimentally if the reaction occurs in a solvent cage. More work is needed to ascertain the involvement of both the singlet and triplet states of the 16-electron fragment. It could well be that our concern about the possible presence of reactive singlets and triplets is unnecessary. Spin–orbit coupling is expected to be substantial for the heavy Ir center and would wash out differentials based on singlet, triplet distinctions.

The Vinyl Hydride → η^2-Olefin Conversion

The sequence to be discussed in this section is that shown in **16**, taking the vinyl hydride complex to the η^2-olefin adduct. There is clearly a substantial amount

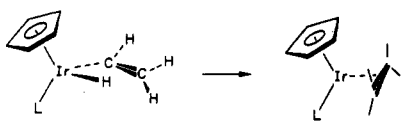

16

of atomic motion involved in the rearrangement, and an optimization of the geometrical parameters corresponding

(18) Veillard, A.; Dedieu, A. *Theor. Chim. Acta* **1983**, *63*, 339.
(19) Dedieu, A., private communication.

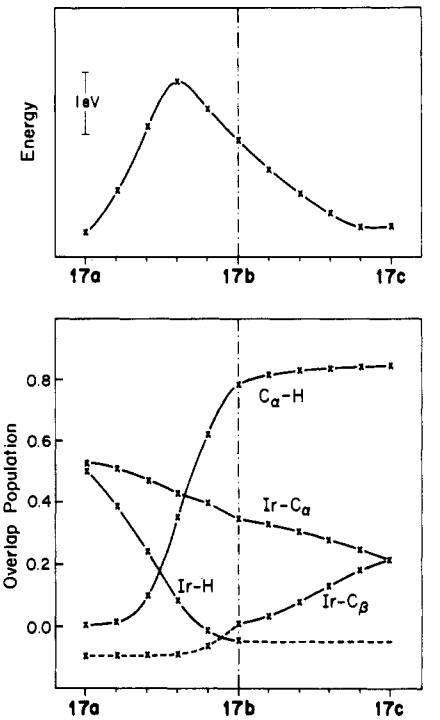

Figure 7. Top: relative energy for the **17a** ↔ **17c** isomerization. Bottom: selected overlap populations going from **17a** to **17c**.

to all the degrees of freedom is computationally out of reach. The calculations described next aimed rather at a semiquantitative evaluation of the isomerization and at an understanding of how the process does take place at all. Experimentally the reaction must be associated with a fairly high activation energy since it proceeds at temperatures of ~170 °C.

A concerted mechanism in which the bonds to be broken are dismantled in *unison* and coupled to all the remaining geometrical parameters was tested numerically, starting from the three orientations generated in **10a–c**. The barrier in each case is high, ~100 kcal/mol, and suggested that things must happen in a somewhat more stepped fashion. The idea was then to break the Ir–H bond while some good Ir–carbon bonding was maintained. Starting from the perpendicular orientation **17a**, we tried a hydrogen transfer ending up in a geometry, **17b**, akin to that of an η^1-slipped olefin, which then rotates and readjusts to the η^2-binding mode **17c**. Figure 7 shows the energy diagram for this sequence as well as the variation of a few selected overlap populations. The reaction coordinate consists of two steps (**17a** → **17b**; **17b** → **17c**) separated by the vertical dashed line. The computed transition state lies just before the η^1-olefin geometry, at an activation energy of ~55 kcal/mol starting from the vinyl hydride. The initial step consists of a concomitant migration of the hydrogen to C_α, a repositioning of the Ir–C_α bond in the *yz* plane, a slight rehybridization at C_α, and a rotation of the bottom CH_2 unit so that it eventually ends up perpendicular to *yz*.

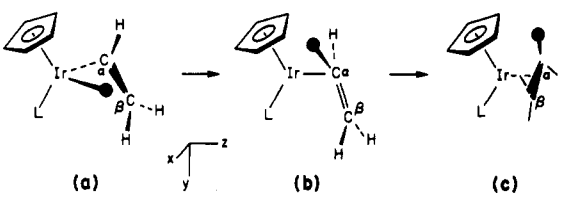

17

Please note the reasonably smooth aspect of the curves; as usual we gain some confidence in the transit constructed

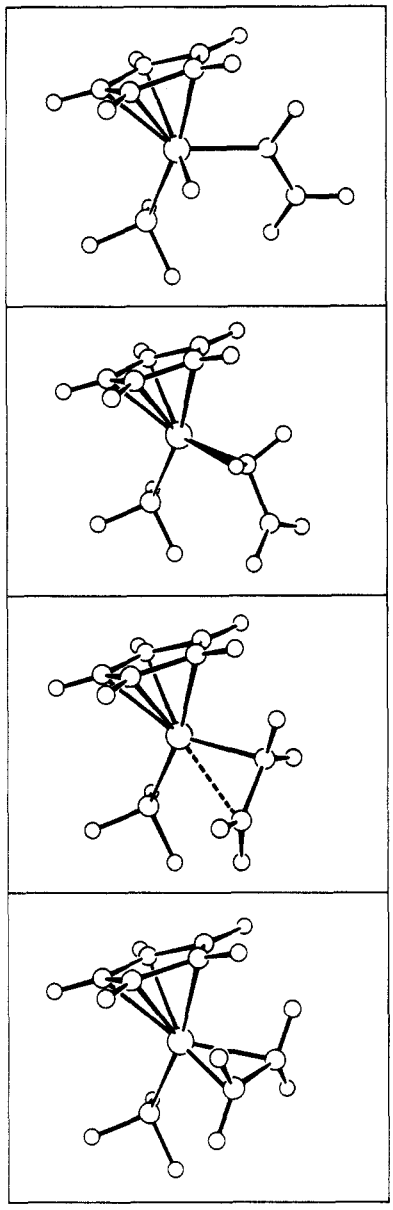

Figure 8. Snapshots of the computed reaction path for the vinyl hydride to complexed ethylene reaction.

from that smoothness. Also it is interesting that the Ir–C_α bond is weakened to the same extent in each of the two steps. The Ir–H and C_α–H curves tell us that a lower activation energy may result if C–H bonding is turned on a little bit faster with respect to the Ir–H bond rupture.

The path **17a–c** just described, shown in a series of snapshots in Figure 8, is the lowest energy one that we could find. The same idea of an η^1 geometry as a rough midpoint was tested starting from different vinyl hydride conformations, but in all cases a much larger energy expenditure was required to proceed to the η^2-bound system. The reason is qualitatively a simple one; some Ir–C_α bonding must be maintained through the whole sequence. The π system via its lobe on C_α allows this feature, since an interaction with 3a′ exists all the way to the η^1 species. This, incidentally, is closely related to an analysis of the nucleophile addition to complexed olefins previously carried out by one of us.[20] A look at the evolution of the net charges on the β-carbon in the initial step (**17a** → **17b**) shows a buildup of positive charge at this center; this leads us to believe that a trapping of the suggested η^1 species by a nucleophile may be observable experimentally.

We now digress briefly and would like to point out that the initially metal-bound hydrogen could conceivably migrate to the β-carbon rather than the α one. The outcome is a fine 18-electron alkylidene complex, **18**. Al-

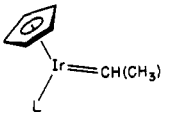

18

though interconversion between η^2-olefins and alkylidenes has some precedent in the literature,[21] we should hasten to say that **18** is not likely to be a point connecting the vinyl hydride to the olefin complex: a large activation energy is computed for migrating the hydrogen to C_β in **17a** (~3 eV). **18** is computed without geometry optimization to be almost as stable as the olefin complex. The synthesis of **18** via a different route would be extremely interesting. Complementary information would be gleaned since one could investigate the behavior of **18** under the reaction conditions used for the processes discussed here.

Returning to the sequence **17a–c**, we have examined the effects of substituents on the activation energy. Replacing the phosphine ligand by a π acceptor (CO) or a π donor (Cl^-) resulted in minor changes in the energetics of the system. Different R groups on the β-carbon of the olefin were also tried, and we find that whereas Cl^- does not alter in any way the process, a cyano group (CN^-) does lower the activation energy by ~0.5 eV. This was somewhat surprising since on going from the vinyl hydride **17a** to the η^1-olefin **17b** the α-carbon grows slightly positive. Although we cannot propose an explanation for this at the moment, an experimental test could tell whether our intuition or the computational technique is at fault here.

The reader will have realized that our conclusions so far have been based on calculations carried out only for a *model* of the real material: the methyl groups on both the Cp ring and the phosphine have been substituted by hydrogens.

In the next section we embark on an analysis of the steric factors upon the overall potential energy surface.

Role of the Steric Factor

To understand and measure fully the extent to which the real system is hindered, one can recalculate a potential surface analogous to that of Figure 3, but now putting five methyl groups on the cyclopentadienyl and three on the phosphine. That figure indicates in a two-dimensional graph the way the bending of the ligands and the dihedral angle made by the C–C double bond in the vinyl–hydride system (see **6**) affect the energy of the system. The new picture featuring methyl groups in due places is the object of Figure 9. The conventions are the same as those used for Figure 3. It is instructive to compare the two figures. The high-energy regions have "grown" dramatically, making the potential around the two minima (filled and empty circles) harder, steeper. Basically, there is left only one channel to interconvert the two minima, corresponding roughly to geometries **10b** and **10c**. The transition state for this process is depicted in **19**. It lies ~30 kcal/mol above the global minimum—recall it cost only ~10 kcal/mol in the model system to undergo rotation around the Ir–C_α bond. We should note that in Figure 7 the numbers appended to the contours are in kilocalories per mole and again refer to the energy zero of a fully disso-

(20) Eisenstein, O.; Hoffmann, R. *J. Am. Chem. Soc.* **1981**, *103*, 4308.

(21) Theopold, K. H.; Bergman, R. G. *Organometallics* **1982**, *1*, 219.

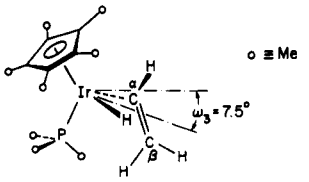

19

ciated Cp^*IrL^*/C_2H_4 system ($Cp^* = C_5Me_5$; $L^* = PMe_3$). Also it is worth mentioning that the two minima lie at the same energy, within 1 kcal/mol. The X-ray structure of the isolated vinyl hydride[10] shows it to be very close to the empty circle of Figure 7, at least in terms of the two restricted parameters defining the surface.

It is clear from the sharp potential around $\theta = 0°$ that the path we had accepted for the model system, as far as the oxidative addition step is concerned, **10a**, must be reconsidered. In particular, it is doubtful if the vinyl fragment will enter and end in an upright conformation, as suggested by electronic factors only. Steric hindrance will make the C_2H_3 unit rotate along the reaction path. In other words, the transition state for the oxidative addition is likely to feature a C_2H_3 unit with an orientation θ such that $0° < |\theta| < 90°$. A further consequence of the bulk around the metal is that the C–H bond will have to cleave before the minimum distance d of 1.8 Å can be attained in the upright orientation. To be on the safe side and still get a feeling for the change in the activation energy, an oxidative addition reaction path was computed starting at $d = 2.0$ Å, $\omega_3 = 0°$, and $\theta = 0°$ and ending at one of the two best vinyl hydride structures of Figure 9, that with $\theta = 270°$ and $\omega_3 = 18°$. The barrier is now 36 kcal/mol. Clearly, due to the assumptions made in our devising this transit, the actual value is likely to be somewhat less. The influence of the steric bulk is therefore not that much on the barrier per se but rather on the topology of the reaction: for the C–H oxidative addition, the electronic and steric demands go in opposite direction—the former favor an upright insertion (**10a**), whereas the latter rather tends to force the ethylene into parallel geometries. However, despite this geometrical constraint, the orientation of the incoming ethylene is still relatively flexible—the angle θ really matters late in the process.

Earlier in the text we mentioned that the competition existing between the C–H oxidative addition and the direct addition of C_2H_4 to the 16-electron unit could come about for a reason other than the difference in the spin states of the species involved. We would like to suggest here that the entropy contribution to the activation energy is much larger for the ethylene insertion than from the vinyl hydride formation and that this difference arises from the limitations on access to reactive trajectories, i.e. steric constraints at the metallic site. In order to test this idea, we performed a series of calculations which bring the ethylene toward the iridium at a variable angle, ω_1; see **20**.

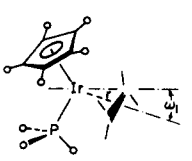

20

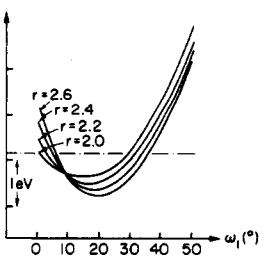

21

In **21** we show schematically the shape of the energy curves

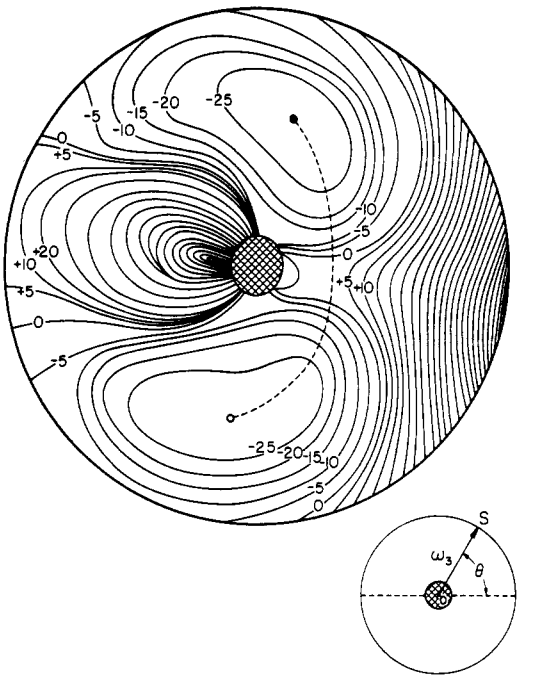

Figure 9. A two-dimensional potential surface optimizing the geometry of the vinyl hydride in its full representation. See text and Figure 3.

obtained by varying ω_1 for a fixed value of r, the distance between Ir and the C–C midpoint. The zero of energy is arbitrary in **21**. The calculations were performed with a planar olefin, and the dashed line of **21** refers to the binding energy.

The plots of **21** tell us the obvious: The further away the olefin the less bound it is—compare the minima. There is more to **21**, though. In particular, clearly displayed is the acuteness of the angle which allows the approach of the olefin. For example at $r = 2.2$ Å, the "window" is only about 25° wide. The bulk of the ligands (C_5Me_5 and PMe_3) forces a very narrow channel in space that the ethylene can and must follow if it is to bind, even though the approach along the best trajectory defined by the curves in **21** has zero activation enthalpy. It is difficult to quantify the effect of constrained access in the absence of trajectory calculations, but we have a feeling that it will be worth a few kilocalories per mole in the free energy of activation.

Up to now, we have discussed the influence of the steric bulk upon reactions 1 and 2 of Scheme I presented in the Introduction. Calculations were performed on the vinyl hydride → η^2-olefin step as well, using Cp* and L*. The path used is that of **17**, but with ω_2 (see **3**) set at 5°; the reason for this choice is found in Figure 9. This value of ω_2 corresponds to the lowest energy point for $\theta = 0°$, i.e., the upright conformation of **17a**. From there, it costs again ~50 kcal/mol to generate the η^2-olefin complex. There is basically no difference between this value and that obtained by using the model unmethylated system for this step. What forced the choice of the perpendicular conformation ($\theta = 0°$) as a starting point is the higher computed activation energy associated with overall rearrangement if one began it from the lowest energy conformation of the vinyl hydride. The sequence of events implicitly defined therefore involves a rotation of the vinyl group from the ground-state geometry to the upright conformation and *then* migration to the η^1-slipped olefin, which eventually collapses to the product. The essential difference between the model and the real system comes about in the initial rotation which costs ~10 kcal/mol in the former and ~30 kcal/mol in the latter.

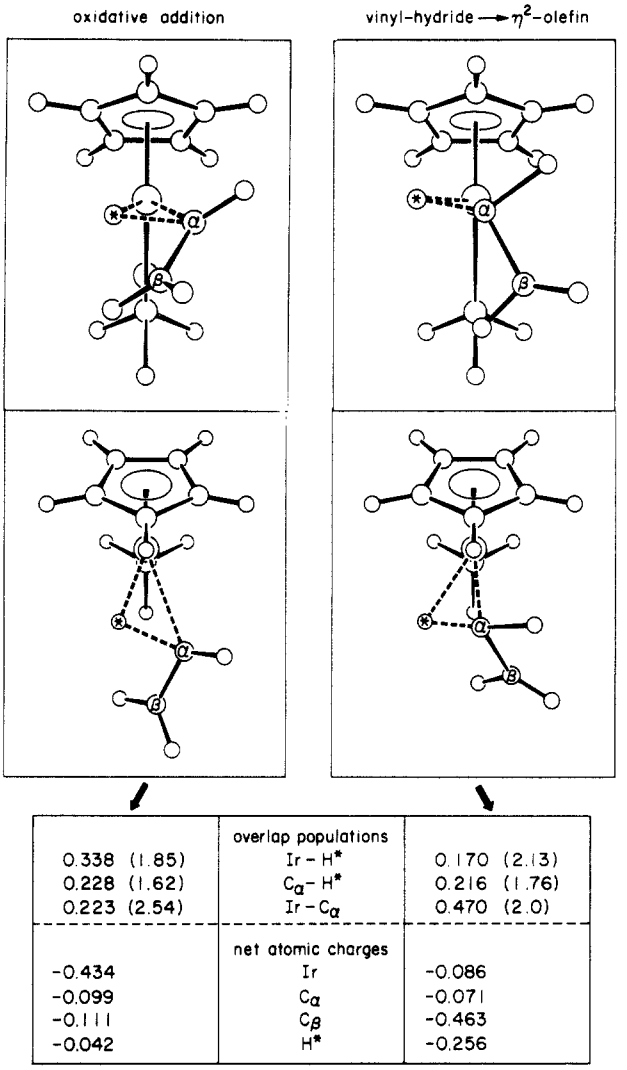

	overlap populations	
0.338 (1.85)	Ir - H*	0.170 (2.13)
0.228 (1.62)	C_α - H*	0.216 (1.76)
0.223 (2.54)	Ir - C_α	0.470 (2.0)
	net atomic charges	
-0.434	Ir	-0.086
-0.099	C_α	-0.071
-0.111	C_β	-0.463
-0.042	H*	-0.256

Figure 10. A geometrical and numerical comparison between the transition states of the vinyl hydride to η^2-olefin reaction (right) and the C–H oxidative addition (left). The top views are along the y axis while the bottom ones are from the $x = 0$, $z > 0$, $y < 0$ quadrant; see text. Numbers in parentheses refer to the corresponding interatomic separations in angstroms.

Discussion and Conclusion

The reader will notice that the results discussed in the previous section indicate a major deficiency in our computational analysis of the proposed scheme. From the ground-state vinyl hydride we compute a smaller activation energy for reductive elimination of C_2H_4 than for migration and interconversion to the olefin complex. The major reason for this state of affairs lies in the relatively large computed barrier to shifting the hydrogen to the α-vinylic carbon (**17a** → **17b**). Recall the one-dimensional transit used for this step. This problem necessarily impinges on our ability to ascertain the existence of two different transition states, one for the vinyl hydride formation and the other for the vinyl hydride to η^2-olefin conversion.

The experimental results[10] clearly show that two such distinct transition states exist. Do our calculations indicate the same? Figure 10 compares the geometries of the two computed transition states, in two views, and indicates various bonding characteristics for them. We think that the two are distinct, for the following reasons: (i) geometrically, the two computed transition states, ③ in Figure 5 and that of Figure 8, differ in both the Ir–C_α distances (2.54 and 2.0 Å, respectively) and in the orientation of the C–C double bond (upright in one case, tilted in the other); (ii) as a consequence of the above, the electronic structure of the system at these two points is different as well: in the C–H oxidative addition process, the Ir–C_α bond is incipient at the transition state, whereas the same bond must keep most of its strength while the hydrogen migrates and the η^1-olefin geometry is attained. A close examination of the charge distribution at the two points also reveals a number of differences, not all of them being easily explainable.

Table II. Extended Hückel Parameters

orbital	H_{ii}, eV	ζ_1	ζ_2[a]	C_1	C_2[a]
Ir 5d	-12.1	5.796	2.557	0.6351	0.5556
6s	-11.36	2.504			
6p	-4.5	2.20			
P 3s	-18.6	1.6			
3p	-14.9	1.6			
C 2s	-21.4	1.625			
2p	-11.4	1.625			
H 1s	-13.6	1.3			

[a] Exponents and coefficients in the double-ζ expansion.

Of course we realize that the dissimilarities between the two points could be introduced by the choice of our reaction coordinates. The only way the question can be settled would be with better calculational procedures and complete geometry optimization.

The existence of two transition states would be mandatory within the standard framework of transition-state theory, given the experimental results.[10] But who knows, perhaps we are reaching the limits of transition-state theory here. Perhaps the same thing is happening here as for many possibly concerted reactions with partial but not exclusive stereoselectivity. In these a transition-state mode of analysis leads to the postulation of competing concerted and diradical pathways. But we suspect that these reactions are telling us rather that we have overextended the remarkably useful transition-state model and that we should really be doing collison theory. It could be that there is only one pass on the surface and that the intricacies of the approaches to that pass, which can only be explored with trajectory calculations, lead to two different reaction cross sections, i.e., rate constants. A similar philosophy underlies the incisive recent considerations of Carpenter.[22]

In this contribution we have tried to understand and describe some of the behavior of the $CpIrL/C_2H_4$ system. The three reactions observed experimentally have been investigated by means of computations at the extended Hückel level. The way the steric factors shape the overall potential surface have been analyzed in some detail. They influence drastically the geometric flexibility of the vinyl hydride and the access of the olefin to the metal but do not seem to alter the electronics of the various reactions examined.

While we have learned much in the course of this study, it is clear that the limitations of the extended Hückel method in computing potential energy surfaces do not leave us with the feeling that the reaction is satisfactorily modeled by the theory, at least at the level we have been able to apply it. We point once again to the much too high computed activation energy for the vinyl hydride to olefin rearrangement as a conspicuous deficiency. Better calculations are needed. The reaction retains some mystery.

Acknowledgment. We are grateful to the National Science Foundation for the support of its work through

(22) Carpenter, B. K. *J. Am. Chem. Soc.*, in press.
(23) Dubois, D. L.; Hoffmann, R. *Nouv. J. Chem.* **1977**, *1*, 479.

Grant CHE84-06119, and to the Council for International Exchange of Scholars for making M.J.C.'s stay at Cornell possible.

Appendix

The computations used the extended Hückel method with H_{ii}'s and other relevant parameters listed in Table II. The off-diagonal elements were evaluated with the weighted H_{ij} formula.[24]

The C–C, C–H, Ir–centroid, P–H, and Ir–P bond distances were set at 1.41, 1.1, 1.724, 1.42, and 2.42 Å, respectively. The H–Ir–C_α bond angle in the vinyl system was kept at 80.0°. The Ir–P–H angle were set at 123.1°.

Registry No. C_2H_4, 74-85-1.

(24) Ammeter, J. H.; Bürgi, H.-B.; Thibeault, J. C.; Hoffmann, R. *J. Am. Chem. Soc.* **1978**, *100*, 3686.

Fluxional Exchange of *tert*-Butyllithium Tetramers from Temperature-Dependent ^{13}C–^{6}Li Coupling[1]

Ruthanne D. Thomas,* Matthew T. Clarke, Randy M. Jensen, and T. Corby Young

Center for Organometallic Research and Education, Department of Chemistry, North Texas State University, Denton, Texas 76203

Received December 2, 1985

^{13}C and ^{6}Li NMR studies have been carried out on *tert*-butyl- and *tert*-pentyllithium-^{6}Li in cyclopentane solution. The proton-decoupled ^{13}C resonance for the α-carbon of *tert*-butyllithium-^{6}Li varies from a sharp nine-line multiplet above −5 °C, $J(^{13}C–^{6}Li)$ = 4.1 Hz, to a sharp seven-line multiplet below −22 °C, $J(^{13}C–^{6}Li)$ = 5.4 Hz. This indicates slowing of the fluxional exchange of the *tert*-butyllithium tetramer at low temperatures. A line-shape analysis of the ^{13}C and ^{6}Li exchange-broadened spectra yields activation parameters for the fluxional exchange of $\Delta H^{\ddagger}$ = 25.0 ± 0.1 kcal/mol and $\Delta S^{\ddagger}$ = 44 ± 1 eu. In contrast, the α-carbon of *tert*-pentyllithium-^{6}Li is a temperature-independent nine-line multiplet with $J(^{13}C–^{6}Li)$ = 4.0 Hz. This is interpreted in terms of a similar fluxional process with $\Delta G^{\ddagger}$ (188 K) ≤ 7.9 kcal/mol. The possible mechanisms for fluxional exchange are discussed.

Introduction

It is well-known that alkyllithium compounds exist as aggregates, $(RLi)_n$, where n depends on the alkyl group, solvent, concentration, and temperature.[2] Aggregation states of alkyllithium compounds in hydrocarbon solvent range from dimers[3,4] to octamers and nonamers,[5] with the majority of compounds existing primarily as tetramers, I, and hexamers, II. These compounds undergo a variety

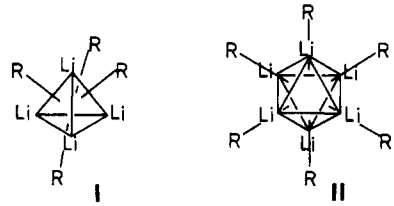

I

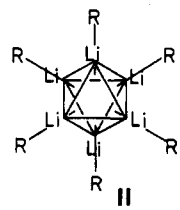

II

of exchange processes in solution including inversion at carbon bonded lithium, interaggregate carbon–lithium bond exchange, and intraagregate carbon–lithium bond exchange. While NMR studies have revealed many details of inversion at carbon and interaggregate exchange,[6,7] much less is known about the mechanism of intraaggregate exchange (fluxionality).

Lithium aggregates have been observed at both the fast and slow fluxional exchange limits in hydrocarbon solvent.[4–8] In general, the presence of fluxionality has been established on the basis of the multiplicity of the ^{13}C NMR resonance of the α-carbon due to carbon–lithium coupling[8,9] or, where the entire multiplet could not be seen, from the value of the observed coupling constant.[5] Evidence for the slowing of the fluxional character of *tert*-butyllithium has also come from the ^{7}Li NMR spectra of mixtures of *tert*-butyllithium and [(trimethylsilyl)-methyl]lithium.[10] On the basis of these studies, hexamers are apparently fluxional under all conditions, while tetramers exchange more slowly. The presence of empty sites on the octahedral hexamer has been proposed as a possible explanation for the higher fluxional rate of hexamers relative to tetramers,[7] although details of the mechanism for fluxional exchange are unknown.

Information on the energetics and mechanism of fluxionality would be particularly useful in understanding the mechanistic details of the reactions of alkyllithium aggregates with other compounds. It is likely that the rate-determining step for some of the reactions of alkyllithium compounds with other substrates is related to the fluxional process. Brown very early suggested[10] that the

(1) Presented in part at the 189th National Meeting of the American Chemical Society Miami, FL April 1985; paper INOR 69.

(2) (a) Wardell, J. L. *Comprehensive Organometallic Chemistry*; Wilkinson, G., Stone, F. G. A., Abel, E. W., Eds.; Pergamon: Oxford, 1982; Vol. 1 pp 43–120. (b) Wakefield, B. J. *The Chemistry of Organolithium Compounds*; Pergamon: Oxford, 1974.

(3) Glaze, W. H.; Freeman, C. H. *J. Am. Chem. Soc.* **1969**, *91*, 7198–7199.

(4) Fraenkel, G.; Henrichs, M.; Hewitt, M.; Su, B. M. *J. Am. Chem. Soc.* **1984**, *106*, 255–256.

(5) Fraenkel, G.; Henrichs, M.; Hewitt, J. M.; Su, B. M.; Geckle, M. J. *J. Am. Chem. Soc.* **1980**, *102*, 3345–3350.

(6) (a) Witanowski, M.; Roberts, J. D. *J. Am. Chem. Soc.* **1966**, *88*, 737–741. (b) Fraenkel, G.; Beckenbaugh, W. E.; Yang, P. P. *J. Am. Chem. Soc.* **1976** *98*, 6878–85.

(7) Fraenkel, G.; Hsu, H.; Su, B. M. *Lithium, Current Applications in Science, Medicine, and Technology*; Bach, R. O., Ed.; Wiley: New York, 1985; pp 273–289.

(8) Bywater, S.; Lachance, P.; Worsfold, D. J. *J. Phys. Chem.* **1975**, *79*, 2148–2153.

(9) Seebach, D.; Amstatz, R.; Dunitz, J. D. *Helv. Chim. Acta* **1981**, *64*, 2622–2626.

(10) Hartwell, G. E.; Brown, T. L. *J. Am. Chem. Soc.* **1966**, *88*, 4625–4629

0276-7333/86/2305-1851$01.50/0 © 1986 American Chemical Society